

Effects of modified hyperbranched polyester as a curing agent on the morphology and properties of dynamically cured polypropylene/polyurethane blends

NAI XU, WENFANG SHI*

State Key Laboratory of Fire Science and Department of Polymer Science and Engineering, University of Science and Technology of China, Jinzhai Road 96, Hefei Anhui 230026, People's Republic of China

E-mail: wfshi@ustc.edu

MING GONG, JIANPING FENG

Laboratory of Mechanical and Material Science, University of Science and Technology of China, Jinzhai Road 96, Hefei Anhui 230026, People's Republic of China

Published online: 21 April 2006

The dynamic vulcanization process, usually used for the preparation of thermoplastic elastomers, has been applied to prepare polypropylene (PP)/polyurethane (PU) blends. Boltorn™ H20 (H20) hyperbranched polyester containing 16 hydroxyl end groups and pentaerythritol are used as curing agents, respectively, for curing PU oligomer during blending with molten PP. To improve the compatibility of cured PU particles with PP matrix, H20 is partly functionalized with stearic acid. The morphology, mechanical properties, thermal properties and melt flow index (MFI) of the PP/PU blends with different curing agent are investigated. Compared with pentaerythritol, SEM photographs show that H20 partly functionalized with stearic acid effectively reduces the size and size distribution of cured PU particles in PP/PU blends which also is proved by MFI measurement. Consequently, the dynamically cured PP/PU blends with modified H20 have better mechanical properties than those cured with pentaerythritol. The shifts of crystallization peaks to higher temperatures for all PP/PU blends indicate that PU particles in the blends can act as effective nucleating agents. Moreover, due to the smaller size of PU particles PP/PU blends cured with modified H20 have higher crystallization temperatures than those blends cured with pentaerythritol at the same PU content. © 2006 Springer Science + Business Media, Inc.

1. Introduction

Dynamic vulcanization is the process for vulcanizing elastomers *in situ* during melt mixing with molten thermoplastics, and the obtaining production is called thermoplastic vulcanizates [1–3]. Thermoplastic vulcanizates combine the excellent processing performance of thermoplastics with the elastic properties of elastomers [4–6]. A large number of elastomers and thermoplastics have been introduced to produce thermoplastic vulcanizates with dynamic vulcanization, such as nitrile rubber (NBR)/poly(vinyl chloride) (PVC) [7], NBR/polyamide (PA) [8], nature rubber/polypropylene (PP) [9], and

ethylene-propylene- diene terpolymer (EPDM)/PP [10]. Many researches have concerned on the dynamic vulcanization of elastomers in molten plastics. However, there are very few publications concerning dynamic vulcanization applied to thermosetting resin/thermoplastic systems.

PP has become the fastest growing plastic because of its versatility, wide applicability, and low cost. However, its defect of brittleness restricts further application of PP. In 1984, it was first reported by Kurauchi [11] that the addition of rigid organic particles could improve the toughness of polymeric materials, whereas the tensile strength kept unchanged. To enhance the toughness of a material,

*Author to whom all correspondence should be addressed.

it is necessary to increase the energy absorption in the matrix that can be achieved through various deformation mechanisms before a failure occurring and during crack propagation. The most effective toughening mechanism is induced by the addition of a second phase in the form of particles. Whatever their nature and properties, there are also many other factors that can influence on the toughening effect of rigid organic particles, including their size, interparticle distance, particle/matrix interaction, and volume fraction. One possible toughening mechanism of rigid organic particles is thought to be that the disperse phase is deformed in a cold-drawing, which is caused by the difference between the elastic modulus of a dispersion phase and a matrix.

Hyperbranched polymers have attracted significant interests due to their promising architecture and properties, such as globular structures and a large number of functionalized end groups, and low viscosity and high solubility. Those properties make them attractive in many applications including coatings, additives, catalysts and nonlinear optics [12–14]. Recently, a few studies reported on the applications of hyperbranched polymers for modifying semi-crystalline polymers. Hong *et al.* [15] demonstrated that the addition of hyperbranched polyester (HBP) to linear low-density polyethylene (LLDPE) successfully eliminated surface defects in the normal tubular film blowing process, with no significant changes on overall physical properties. Moreover, the processibility of blends was improved significantly through the addition of HBP. Jannerfeldt *et al.* [16] reported that the interfacial adhesion between fusion bonded plaques of PP and PA6 strongly increased with the addition of hyperbranched polyester grafted-PP (PP-HBP) in contrast with the same level of maleic anhydride (MAH) grafted-PP (PP-MAH). It is explained by higher concentration of reactive sites in a HBP molecule that allows more PA6 molecules to be grafted with the HBP at the interface. Because multiplayer film extrusion processes require a high compatibiliser diffusivity to obtain a strong interfacial adhesion within a short processing time, PP-HBP which has high diffusivity and functionality, can advantageously be used for those processes allowing the use of less compatibilisers or faster processing rates.

In this study, because of the multi-hydroxyl end groups, hyperbranched aliphatic polyester Boltorn™ H20 was introduced as a curing agent to dynamically cure polyurethane (PU) oligomer in PP blend system. It is well known that PU is incompatible with PP. So Boltorn™ H20 was thus partly functionalized with stearic acid to improve the compatibility of cured PU particles with PP matrix. For comparison, pentaerythritol was used as another curing agent. The size and dispersion of cured PU particles in PU/PP blends with different curing agents were observed by scan electron microscopy (SEM). And in order to study the toughening effect of cured PU particles, the mechanical properties, melting parameters and

crystallinity of PU/PP blends with different curing agent were determined.

2. Experimental

2.1. Materials

PP (F401) was purchased from Yangzi Petrochemical Co. Ltd. (China), with a melt-flow index of 1.9 dg/min (230°C, 2.16 kg). Hyperbranched aliphatic polyester Boltorn™ H20 (H20) [17], theoretically having 16 hydroxyl groups per molecule, was supplied from Perstorp AB, Sweden. Antioxidant, tetrakis[methylene(3,5-di-*t*-butyl-4-hydroxyhydrocinnamate)]methane (Irganox 1010), was supplied from Ciba Specialty Chemicals AB. Poly(ethylene glycol) (PEG) 1000, toluene, 2,4-diisocyanate (TDI), pentaerythritol (PTT), and stearic acid, and other chemicals were supplied by China Medicine (Group) Shanghai Chemical Reagent Co.

2.2. Synthesis

2.2.1. Synthesis of 50% functionalized H20 with stearic acid (H20M)

50% Hydroxyl end groups of H20 were esterified with stearic acid by acid catalysis and azeotropic removal of water according to a procedure described in the literature [18]. The product is code as H20M.

2.2.2. Synthesis of polyurethane (PU) oligomer with isocyanate (–NCO) end groups

The synthesis of polyurethane (PU) oligomer endcapped with –NCO groups was carried out using a 1:2 molar ratio of PEG 1000 and TDI. PEG 1000 (100 g, 0.1 mol) was dissolved in CH₂Cl₂ and put into a pressure equalizing funnel with 1 g of dibutyl tin dilaurate as catalyst. TDI (34.8 g, 0.2 mol) was contained in a round-bottomed flask. The PEG 1000 solution was added dropwise into TDI under constant stirring at 35°C for around 12 h. The obtained PU oligomer had contained two free –NCO end groups for further reaction.

2.3. Sample preparation

Dynamically cured H20M/PU/PP blends were prepared in an XSS-300 rheomixer with a speed of 64 rpm at 190°C. H20M, PP and Irganox 1010 (the antioxidant concentration was 1.5 mg 1010/g PP) were first blended for 3 min, and then PU oligomer was added. The total blending process lasted about 10 min. Sheet samples were prepared by a compression molding apparatus at 195°C and a pressure of 15 MPa for 10 min and then cooled to room temperature rapidly.

The samples of dynamically cured pentaerythritol (PTT)/PU/PP blends were prepared following the same procedure as H20M/PU/PP blends.

The code names and compositions of the blends used in this study are listed in Table I.

TABLE I Code names and compositions of the blends used in this study.

Blend code	PP (F401) (wt.%)	PU oligomer (wt.%)	Modified hyperbranched H2O (wt.%)	Pentaerythritol (wt.%)
PP	100	–	–	–
H20M0.75/PU3/PP	96.25	3	0.75	–
H20M1.50/PU6/PP	92.50	6	1.50	–
H20M2.25/PU9/PP	88.75	9	2.25	–
H20M3.00/PU12/PP	85.00	12	3.00	–
H20M3.75/PU15/PP	81.25	15	3.75	–
PTT0.05/PU3/PP	96.95	3	–	0.05
PTT0.10/PU6/PP	93.90	6	–	0.10
PTT0.15/PU9/PP	90.85	9	–	0.15
PTT0.20/PU12/PP	87.80	12	–	0.20
PTT0.25/PU15/PP	84.75	15	–	0.25

2.4. Scanning electron microscopy (SEM) images

SEM images of pure PP, PTT0.15/PU9/PP, PTT0.25/PU15/PP, H20M2.25/PU9/PP and H20M3.75/PU15/PP blends were obtained by a Hitachi X-650 scanning microscopy (Hitachi, Japan). The fracture surfaces of specimens were etched with 40% NaOH solution at 80°C for 24 h before coated with gold.

2.5. Mechanical properties

Tensile properties of these PP blends listed in Table I were measured with a Universal Testing Machine (DCS5000, SHMADZU, Japan) in a crosshead speed of 25 mm/min at 25°C. Dumb-bell shaped specimens were prepared according to ASTM D412-87. Notched impact strengths of these blends were measured using an izod impact tester (made in Chengde, China). The dimension of rectangular specimens was 80 × 10 × 4 mm³ with a 45° V-shaped notch (tip radius 0.25 mm, depth 2 mm). The values of the mechanical parameters determined from both tensile and Izod tests were calculated as averages over measurements on five specimens for each composition.

2.6. Thermal behavior

The data of crystallization and melting behavior of the blends were obtained in N₂ atmosphere using a Perkin-Elmer differential scanning calorimeter (model DSC 2). For each test, a 5–6 mg sample was first heated to 200°C at 50°C/min and was then kept at this temperature for 10 min to eliminate previous thermal history. Then the sample was cooled to room temperature at a cooling rate of 10°C/min and then secondly heated to 200°C at a heating rate of 10°C/min for datum collection. The degrees of crystallization of these blends were evaluated from the relative ratios of the values of fusion heat of the blend to the fusion heat of PP ($\Delta H_{pp} = 209$ J/g) [19].

2.7. Melt flow index (MFI)

MFI values of these PP blends were measured at 230°C with a 2.16 kg load according to ASTM D-1238.

3. Results and discussion

3.1. Morphology

Fig. 1 shows SEM micrographs of fracture surface of PP, PTT0.15/PU9/PP, PTT0.25/PU15/PP, H20M2.25/PU9/PP and H20M3.75/PU15/PP blends, respectively. It can be seen that there is no hole existing on the fracture surface of PP specimen, as shown as Fig. 1a. It is known that PP is inert to NaOH solution, so there is no etching happening on Fig. 1a. The fracture surfaces of PTT0.15/PU9/PP blend with 9 wt.% PU and PTT0.25/PU15/PP blend with 15 wt.% PU are shown in Fig. 1b and c, respectively. PP constitutes a continuous matrix in which the cured PU particles with curing agent pentaerythritol dispersed. The PU particles is larger in size with wider size distributions when PU content is 9 wt.%, as shown as Fig. 1b. However, when 15 wt.% PU was added, some PU particles aggregated into irregular shape. Compared with PTT0.15/PU9/PP and PTT0.25/PU15/PP blends, H20M2.25/PU9/PP and H20M3.75/PU15/PP blends with curing agent H20M display significantly finer particle size and narrower particle size distribution of the dispersed phase, as shown as Fig. 1d and e, respectively. Compared H20M2.25/PU9/PP blend (Fig. 1d) with PTT0.15/PU9/PP blend (Fig. 1b) at the same PU content (9 wt.%), Fig. 1d shows that finer cured PU particles with an average diameter of about 1.0 μm are dispersed in the PP matrix. The small particle size should be related to the presence of modified hyperbranched polyester H20 (named as H20M), in which half hydroxyl end groups (theoretically 8 end groups) have been modified into C-18 alkanes by stearic acid. As shown as Scheme 1, when the multi-hydroxyl end groups of H20M react with –NCO end groups of PU oligomer during blending process with molten PP, the crosslinking reaction of PU oligomer happens and then cured PU particles forms in PP matrix. And the C-18 end chains on highly branched polymer H20M can improve the compatibility of PU particles with PP matrix during dynamically curing process that leads smaller size and narrower size distribution of cured PU particles in H20M/PU/PP blends than that of PTT/PU/PP blends. When PU content reaches 15 wt.%, some PU particles aggregate together during the dynamically curing process. As a result, some

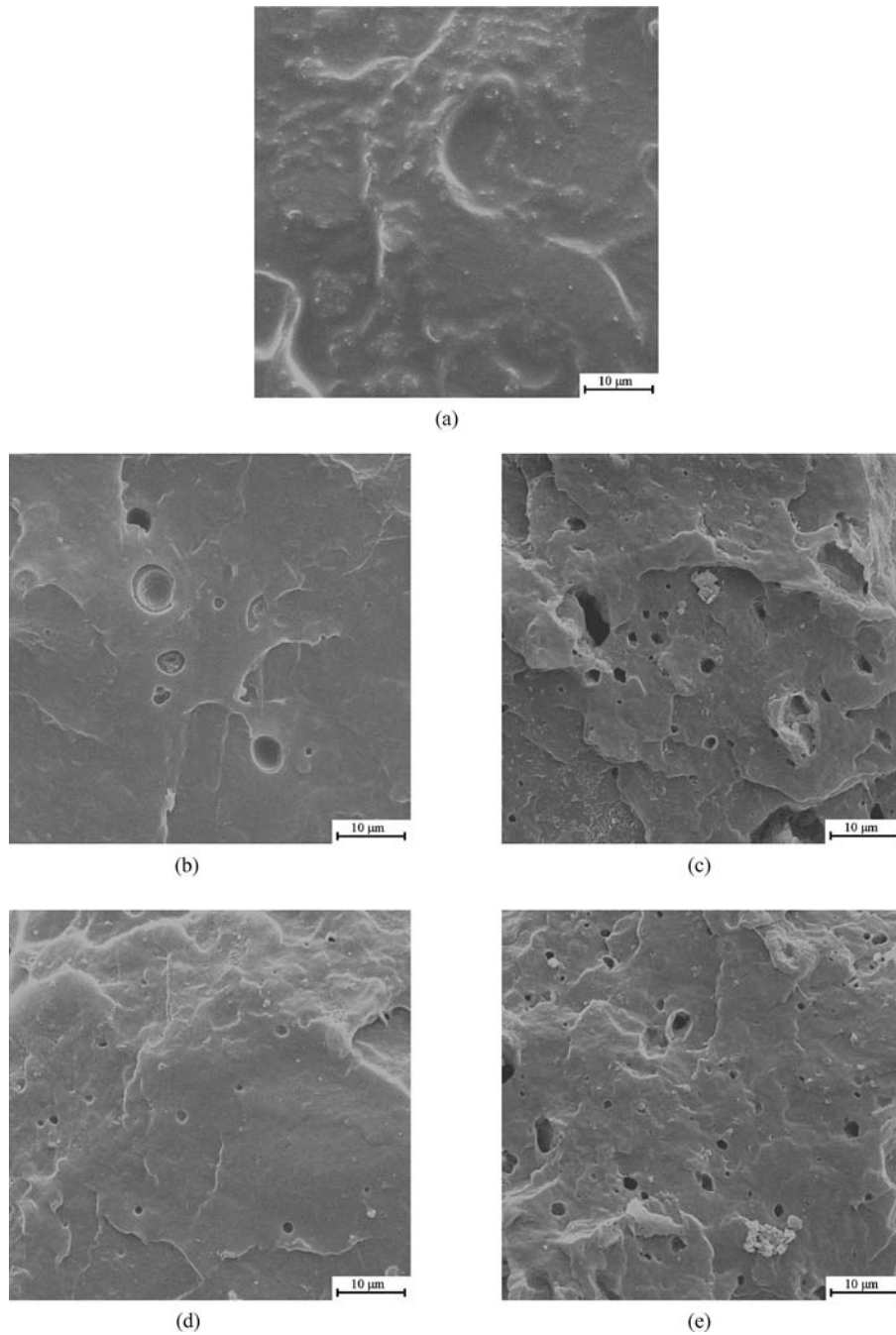


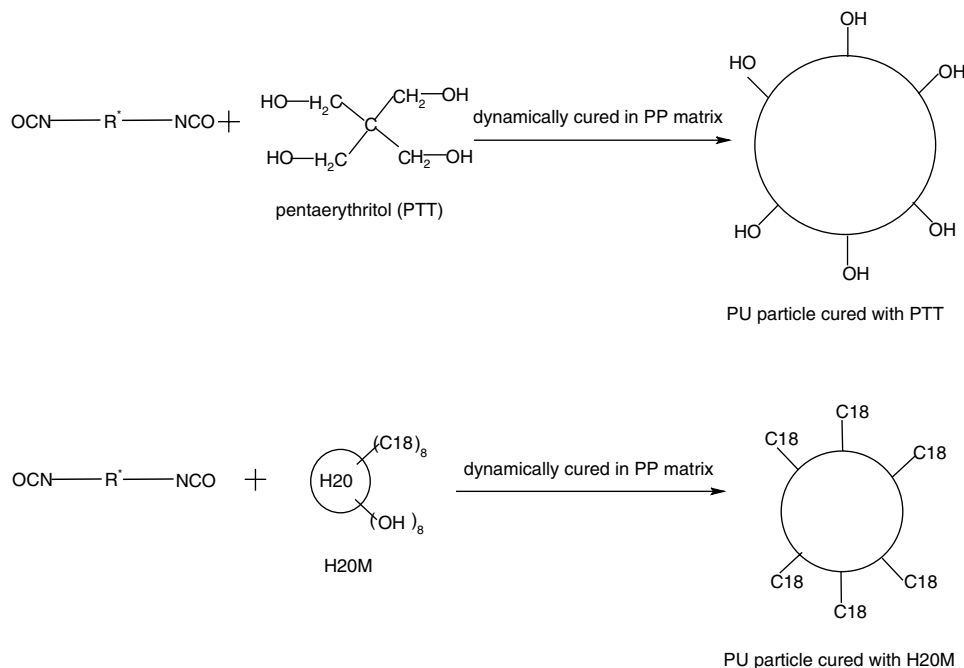
Figure 1 SEM images of fracture surfaces ($\times 2000$): (a) pure PP; (b) PTT0.15/PU9/PP blend; (c) PTT0.25/PU15/PP; (d) H20M2.25/PU9/PP; (e) H20M3.75/PU15/PP blend.

bigger cured PU particles appear in the fracture surface of specimen of H20M3.75/PU15/PP blend.

3.2. Mechanical properties of blends

Table II presents the mechanical properties of H20M/PU/PP and PTT/PU/PP blends. The notched impact strength of blends with different PU contents is shown in Table II. The notched impact strength increases from 4.10 kJ/m^2 for pure PP to 8.96 kJ/m^2 for H20M2.25/PU9/PP containing 9 wt.% PU, and then decreases to 7.89 kJ/m^2 when PU content reaches 15 wt.%.

However, the notched impact strength of PTT/PU/PP blends largely decreases from 4.10 kJ/m^2 for pure PP to 2.51 kJ/m^2 when PU content increases to 15 wt.%. This indicates that addition of a moderate amount of PU and H20M has noticeable effect on the toughness of PP leading the impact strength largely higher than that of pure PP. However, the excess PU addition leads to the decrease of impact strength, which is similar to the experimental results by Yang [20] and Zhou [21]. Compared with H20M/PU/PP blends, the decreases of notched impact strength of PTT/PU/PP blends is due to the incompatibility of PU with PP matrix that leads the PU



Scheme 1 Dynamically curing PU oligomer in molten PP with different curing agents.

TABLE II Mechanical properties of PP, H20M/PU/PP and PTT/PU/PP blends.

Blend code	Notched impact strength (kJm^{-2})	Tensile strength (MPa)	Elongation at break (%)
PP	4.10	43.5	910
H20M0.75/PU3/PP	5.68	43.9	251
H20M1.50/PU6/PP	7.12	44.2	136
H20M2.25/PU9/PP	8.96	44.6	95
H20M3.00/PU12/PP	8.75	42.3	63
H20M3.75/PU15/PP	7.89	40.5	42
PTT0.05/PU3/PP	4.01	42.1	170
PTT0.10/PU6/PP	3.79	40.2	103
PTT0.15/PU9/PP	3.58	37.5	72
PTT0.20/PU12/PP	2.99	36.2	35
PTT0.25/PU15/PP	2.51	34.5	14

particles aggregate together when it is dynamically cured with curing agent PTT in the molten PP (see Fig. 1b and c). However, H20M not only takes the curing react with PU, but also promotes the compatibility of cured PU particles with PP matrix by its multi C-18 end chains leading to a formation of inter-phase between cured PU particles and PP matrix. The SEM photograph of fracture morphology of H20M2.25/PU9/PP (see Fig. 1c) shows that the inter-phase may largely reduce the size of PU particles from $5 \mu\text{m}$ (see Fig. 1b) to $1 \mu\text{m}$ and make them disperse in the matrix homogeneously. Zuiderduin [22] proposed that the rigid particles should be of small size (less than $5 \mu\text{m}$) and disperse homogeneously in the matrix when the toughening effect of polyolefin could be achieved. When the PU content increases from 9 wt.% to 15 wt.% (see Fig. 1d), PU particles trend to aggregate together that leads to the impact strength of H20M/PU/PP blends decrease.

Table II also shows the tensile strength of the H20M/PU/PP blends and PTT/PU/PP blends. The tensile strength of H20M/PU/PP blends almost keeps unchanged when PU content increases from 0 wt.% to 9 wt.%, and then decreases to 40.5 MPa when PU content reaches to 15 wt.%. Compared with H20M/PU/PP blends, Table II also shows a larger decrease in the tensile strength of PTT/PU/PP blends. On the other hand, the elongations at break (%) of all PU/PP blends are much lower than that of pure PP, as shown as Table II. It is also noted that the elongation at break (%) of PPT/PU/PP blend decreases more than that of H20M/PU/PP blends with the same PU contents.

3.3. Melt flow index

The melt flow index (MFI) of H20M/PU/PP and PTT/PU/PP blends with different PU contents are shown in Fig. 2. Compared with PTT/PU/PP blends, the melt flow index (MFI) value of H20M/PU/PP blends shows a larger decrease. It can be seen that the smaller size of PU particles in H20M/PU/PP blends decreases melting viscosity of these blends greater than those of PTT/PU/PP blends. The same result was also observed in the literature [23]. It is also noted that the MFI value of H20M/PU/PP blends shows a faster decrease when PU content increases from 3 wt.% to 9 wt.%, and then keep a slow decrease when PU content reaches to 15 wt.%. The trend shows that the coalescence of PU particles takes place during the dynamically curing process when PU content is more than 9 wt.% in H20M/PU/PP blend.

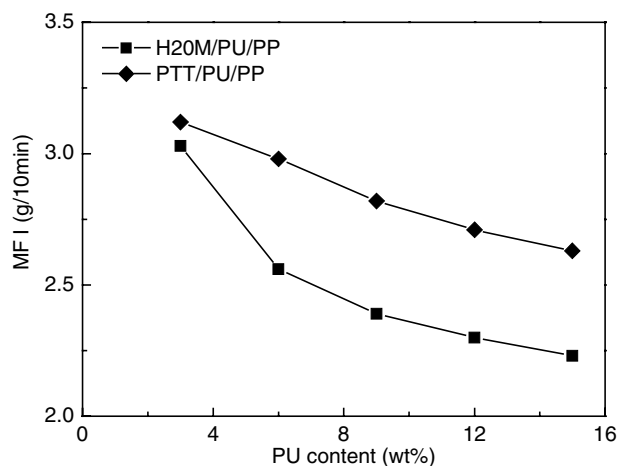


Figure 2 Melt flow index (MFI) for PTT/PU/PP blends and H20M/PU/PP blends with different PU contents.

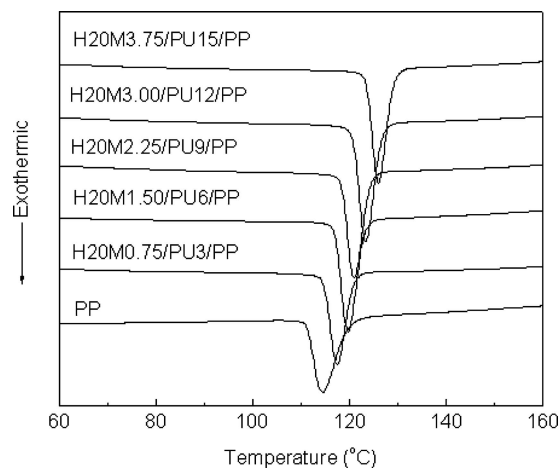


Figure 3 DSC thermograms at the first cooling of PP and H20M/PU/PP blends with different PU contents.

3.4. Crystallization and melting behaviors of blends

PP is a kind of highly crystalline polymer that can crystallize easily even under quenched conditions. Figs. 3 and 4 show the first cooling and second heating DSC scans of PP and its blends with H20M and PU. The thermal properties were determined and characterized by DSC and the data are listed in Table III.

From Fig. 3, it can be seen that all crystallization peak temperatures of H20M/PU/PP blends with PU content from 3 wt.% to 15 wt.% are higher than that of PP (114.7°C). The crystallization peak temperature of H20M3.75/PU15/PP blend with 15 wt.% PU content is higher 11.5°C than that of PP. The shift of crystallization peak temperatures to higher temperature suggests that PU particles in the H20M/PU/PP blends can act as effective nucleating agents and accelerate the crystallization of PP matrix. For studying the effects of PU particle size on the thermal properties of PP blends, Table III also lists the crystallization and melting data of PTT/PU/PP blends with PU content from 3 wt.% to 15 wt.%. From Fig. 1 and Table III, it can be clearly seen that the smaller PU particles due to the presence of H20M in the dynamically cured

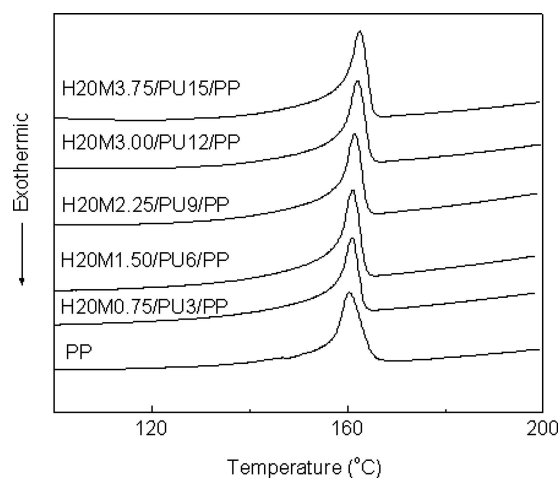


Figure 4 DSC thermograms at the second heating of PP and H20M/PU/PP blends with different PU contents.

TABLE III DSC analysis results for PP, H20M/PU/PP and PTT/PU/PP blends.

Blend code	T_m (°C)	T_c (°C)	Crystallinity (%)
PP	160.5	114.7	43.3
H20M0.75/PU3/PP	160.9	117.6	42.9
H20M1.50/PU6/PP	161.1	119.9	41.1
H20M2.25/PU9/PP	161.5	121.1	39.2
H20M3.00/PU12/PP	162.1	123.6	37.6
H20M3.75/PU15/PP	162.6	126.2	33.9
PTT0.05/PU3/PP	160.4	115.1	43.0
PTT0.10/PU6/PP	160.7	115.8	42.3
PTT0.15/PU9/PP	161.2	116.5	41.7
PTT0.20/PU12/PP	161.6	118.4	40.2
PTT0.25/PU15/PP	161.3	120.8	39.7

T_m -Peak melting temperature; T_c -Peak crystallization temperature.

H20M/PU/PP blends provide more nucleating agents that increase the crystallization peak temperature of PP matrix. A similar result was reported for PP/polycarbonate (PC) blends [24]. PC could act as a nucleating agent and accelerate the crystallization of PP in PP/PC blends. Jiang *et al.* [25] also reported that epoxy particles in PP/epoxy blends could act as effective nucleating agents of PP matrix. The smaller epoxy particles in the blends resulted in an increase of the number of nucleating agent and higher crystallization temperatures of PP matrix. From Table III, the melting temperatures of all PP/PU blends are slightly higher than that of PP (160.5°C). The crystallinities of PP matrix in all PP/PU blends are lower than that of PP. The crystallinity in H20M3.75/PU15/PP blend containing 15 wt.% PU is 33.9%, which decreases by 9.4% compared with that of PP. While for PTT0.25/PU15/PP blend containing 15 wt.% PU the crystallinity also decrease from 43.3% to 39.7%. Van *et al.* [23] reported that EPDM could act as a nucleating agent for PP in PP/EPDM blends. However, the crystallinity decreased at the presence of EPDM, indicating that the nucleating

effect of EPDM did not necessarily imply an increase in the crystallinity. An increase in the melting temperature of PP in the blends was directly related to the size of PP crystals.

4. Conclusions

The dynamically cured PP/PU blends with different curing agents have been prepared. The SEM photographs indicate that the cured PU particles in H20M/PU/PP blends have smaller size and narrower size distribution than that in PTT/PU/PP blends. It leads MFI values of H20M/PU/PP blends to be lower than that of PTT/PU/PP blends. Compared with poor mechanical properties of PTT/PU/PP blends, the mechanical performances of H20M/PU/PP blends are enhanced because of the controlled size and size distribution of PU particles in PP matrix. The impact strength of H20M/PU/PP blends increases from 4.10 kJ/m² for pure PP to 8.96 kJ/m² for H20M2.25/PU9/PP containing 9 wt.% PU, and then decreases slightly to 7.89 kJ/m² when PU content reaches 15 wt.%. Moreover, the tensile strength of H20M/PU/PP blends is slightly lower than that of pure PP. The crystallization peaks move to higher temperatures for all PP/PU blends, indicating that PU particles in the blends can act as effective nucleating agents. The smaller PU particles provide a mass of nucleating agents in PP matrix resulting to higher crystallization temperatures in H20M/PU/PP blends than PTT/PU/PP blends. It can be concluded from these results that, compared with PTT, H20M can effectively improve the compatibility of cured PU particles with PP matrix and reduce PU particle size and size distribution during the dynamically curing process. As a result, better mechanical properties and higher crystallization temperatures of H20M/PU/PP blends have been obtained.

Acknowledgments

This research was supported by National Natural Science Foundation of China under contract/grant number 50233030.

References

1. M. GESSLER, U.S. Patent 3037954 (1962).
2. K. FISHER, U.S. Patent 3758643 (1973).
3. A. Y. CORAN and R. P. PATEL, *Rubber Chem. Technol.* **53** (1980) 141.
4. N. R. LEGGE, G. HOLDEN and H. E. SCHROEDER, in "Thermoplastic Elastomers—A Comprehensive Review" (Hanser Publishers, Munich, Vienna, New York, 1987).
5. G. HOLDEN, N. R. LEGGE, R. P. QUIRK and H. E. SCHROEDER, in "Thermoplastic Elastomers," 2nd ed. (Hanser Publishers, Munich, Vienna, New York, 1996).
6. B. M. WALKER and C. P. RADER, in "Handbook of Thermoplastic Elastomers", 2nd ed. (Van Nostrand Reinhold, New York, 1998).
7. A. Y. CORAN R. P. PATEL and D. WILLIAMS, *Rubber Chem. Technol.* **55** (1982) 116.
8. A. Y. CORAN and R. P. PATEL, *ibid.* **53** (1980) 781.
9. V. SIBY, A. ROSAMMA and K. BABY, *J. Appl. Polym. Sci.* **92** (2004) 2063.
10. H. W. XIAO, S. Q. HUANG and T. JIANG, *ibid.* **92** (2004) 357.
11. T. KURAUCHI and T. OHTA, *J. Mater. Sci.* **19** (1984) 1699.
12. S. W. ZHU and W. F. SHI, *Polym. Int.* **51** (2002) 223.
13. B. VOIT, *J. Polym. Sci. Pol. Chem.* **38** (2000) 2505.
14. Y. D. ZHANG, L. M. WANG, T. WADA and H. SASABE, *Macromol. Chem. Phys.* **197** (1996) 667.
15. Y. HONG, S. J. COOMBS, J. J. COOPER-WHITE, M. E. MACKAY, C. J. HAWKER, E. MALMSTROM and N. REHNBERG, *Polymer* **41** (2000) 7705.
16. G. JANNERFELDT, L. BOOGH and J. A. E. MANSON, *ibid.* **41** (2000) 7627.
17. A. ANILA and W. F. SHI, *Eur. Polym. J.* **39** (2003) 933.
18. E. MALMSTROM, M. JOHANSSON and A. HULT, *Macromol. Chem. Phys.* **197** (1996) 3199.
19. S. H. CHANG, J. I. DONG and C. K. SUNG, *J. Appl. Polym. Sci.* **32** (1986) 6281.
20. W. J. YANG, Q. Y. WU, L. L. ZHOU and S. Y. WANG, *ibid.* **66** (1997) 1455.
21. Q. ZHOU, W. J. YANG, Q. Y. WU and B. YANG, *Eur. Polym. J.* **36** (2000) 1735.
22. W. C. J. ZUIDERDUIN, C. WESTZAAN, J. HUETINK and R. J. GAYMANS, *Polymer* **44** (2003) 261.
23. A. VAN DER WAL, J. J. MULDER, J. ODERKERK and R. J. GAYMANS, *Polymer* **39** (1998) 6781.
24. C. Q. LI, G. H. TIAN, Y. ZHANG and Y. X. ZHANG, *Polym. Test* **8** (2002) 919.
25. X. L. JIANG, Y. ZHANG and Y. X. ZHANG, *J. Polym. Sci. Pol. Phys.* **42** (2004) 1181.

Received 9 March

and accepted 16 August 2005